The 2010 IEEE/RSJ International Conference on
Intelligent Robots and Systems
October 18-22, 2010, Taipei, Taiwan

Friction Compensation in Energy-Based Bilateral Telemanipulation

Michel Franken, Sarthak Misra, and Stefano Stramigioli
University of Twente, Enschede, The Netherlands

***Abstract*— In bilateral telemanipulation algorithms based on time-domain passivity, internal friction in the devices poses an additional energy drain. Based on a model of the friction, the dissipated energy can be estimated and reclaimed inside the energy balance of the control algorithm. As long as the estimate is conservative, passivity of the entire system is maintained. In this paper we consider two types of friction and discuss the influence of two types of measurement noise. Without noise compensation the dissipated energy is largely overestimated. A compensation method based on the probability density of the noise is proposed. This leads to an energy estimate which is always conservative even in the presence of measurement noise and does not require additional filtering. Simulation results are provided that show the increase in obtained transparency when this energy compensation technique is applied.**

I. Introduction

A bilateral telemanipulation system, Fig. 1, presents the user with haptic feedback about the interaction with the remote environment. Such a system is said to be transparent when the user has the perception of direct interaction with the remote environment [8]. This means that the user should not be able to discern the dynamic behavior of the devices and the controllers themselves during operation. When left uncompensated internal mechanical device friction at both the master and slave side can decrease the obtained transparency.

Several model-based friction compensation techniques have been proposed to decrease the negative influence of internal friction on the transparency of the system. Based on a model of the friction an additional force is computed, which is added to the force computed by the controller. This additional force "cancels out" the friction force. Examples considering different friction sources and using different models are the work of Bernstein et al. [2], Hayward et al. [7], and Ferretti et al. [4]. Mahvash et al. [10] present that such techniques can overcompensate the device friction, which is dangerous as this may lead to stability problems. They introduce a compensation technique for tendon-driven joints based on single-state elastic friction models which is guaranteed to be passive and thus overcompensation cannot take place.

The concept of passivity is also used as a design tool for the entire control structure. Passivity is an elegant solution to deal with the destabilizing influence of time delays in the communication channel connecting the master and slave device and hard contacts on bilateral control algorithms.

Michel Franken, Sarthak Misra and Stefano Stramigioli are affiliated with the Institute for Biomedical Technology and Technical Medicine (MIRA). {*m.c.j.franken, s.misra, s.stramigioli*}@utwente.nl

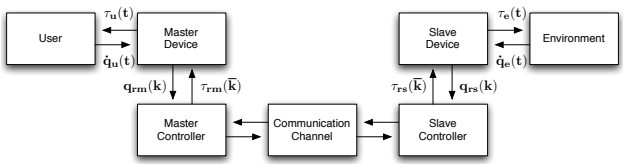

Fig. 1. **Schematic overview of all the components of a bilateral telemanipulation system:** τ_* and $\dot{q}_*$ represent forces/torques and velocities, respectively. The subscripts u, rm, rs and e represent the user, master controller, slave controller, and environment, respectively.

Time-domain passivity architectures have been proposed in literature for impedance-type devices (force as an output causality) which ensure that the telemanipulation system remains passive and thus stable. Two examples are the work by Ryu et al. [11] and Franken et al. [5]. Time-domain passivity of a telemanipulation system implies that all the energy which is extracted from one side, was injected at the other side. These architectures are usually defined on the interconnection of the continuous and discrete domain as at that point the energy exchange can precisely be determined [14]. However, this implies that all the energy which is dissipated due to internal friction in the slave device needs to be injected by the user, irrespective of the chosen control structure. This can severely decrease the level of transparency that can be obtained.

In this paper, we will consider the situation in which the slave device contains a high amount of friction. We will extend the two-layered framework introduced by Franken et al. [5] with a dissipated energy compensation component at the slave side. This energy compensation will increase the transparency of the telemanipulation system as the energy dissipated internally in the slave device no longer has to be injected by the user.

The paper is organized as follows: Section II introduces the two-layered approach to bilateral telemanipulation. Section III presents the used friction model and the compensation strategy. Section IV discusses the noise sensitivity of the compensation strategy described in Section III and introduces adequate measures based on the stochastic properties of the measurement noise to prevent overcompensation. Simulation results showing the improved transparency with this friction compensation technique are presented in Section V. The paper concludes and provides direction for future work in Section VI.

II. Two-Layered approach

In this section we will briefly treat the working of the two-layered framework proposed by Franken et al. [5]. They showed that it is possible to implement a direct energy

coupling between the interaction port at the master and the slave side which is passive irrespective of the time delays present in the communication channel. This energy coupling can be combined with any control strategy to obtain transparency of the system. For a full treatise of the theory behind this framework please refer to [5][1].

The framework consists of two control layers in a hierarchical structure, the *Transparency Layer* and the *Passivity Layer*, see Fig. 2. The *Transparency Layer* can contain any control algorithm that delivers the desired transparency, as long as it results in a desired torque/force to be applied to the devices at both sides. These desired torques are the inputs to the *Passivity Layer*. The *Passivity Layer* is centered around the concept of communicating energy tanks. An energy tank is defined at both the master and the slave side. From these tanks motions by the master and the slave device can be powered and when the available energy is low, the forces which can be exerted by the devices are restricted. A modulated damper is defined at the master side to regulate the energy level in the system. It is activated in order to extract an initial amount of energy, and further additionally required energy, from the user to maintain passivity.

An energy requirement can be detected as the energy level in the tank available during sample period $\overline{k+1}$, $H_m(\overline{k+1})$, will drop below the desired level of the tank, H_d. Such a requirement can be detect at both sides. The additional force, τ_{TLC}, exerted by this modulated damper, $d(k)$, will be

$$\begin{aligned} \tau_{TLC}(k) &= -d(k)\dot{q}_m(k) \qquad (1)\\ d(k) &= \begin{cases} \alpha(H_d - H_m(\overline{k+1})) & \text{if } H_m(\overline{k+1}) < H_d \\ 0 & \text{otherwise} \end{cases} \end{aligned}$$

where $\dot{q}_m(k)$ is the velocity of the master device at sample instant k and α is a tuning parameter for the rate at which the additional required energy is extracted from the user.

The energy exchange, $\Delta H_I(k)$, between the continuous and discrete domain for impedance type displays can be exactly computed *a posteriori* as

$$\begin{aligned} \Delta H_I(k) &= \int_{(k-1)T}^{kT} \tau_{rm}(\overline{k})\dot{q}_{rm}(t)dt \\ &= \tau_{rm}(\overline{k})\Delta q_{rm}(k) \qquad (2) \end{aligned}$$

where $\tau_{rm}(\overline{k})$ is the force applied by the actuators during sample period $\overline{k}$, $\dot{q}_{rm}(t)$ is the velocity at which the actuators are moving, and $\Delta q_{rm}(k)$ is the change in position of the actuators measured at sample instant k. .

The *Passivity Layer* contains an algorithm which monitors and enforces the neutral energy balance of the system:

$$\Delta H_T(k) = \Delta H_{Im}(k) + \Delta H_{Is}(k) \qquad (3)$$

where $\Delta H_{Im}(k)$ and $\Delta H_{Is}(k)$ are the amounts of energy exchanged between the continuous and discrete domain at the master and slave side during sample period $\overline{k}$, respectively. $\Delta H_T(k)$ is the change at sampling instant k of the energy present in the *Passivity Layer*, $H_T(\overline{k})$. In [5] the algorithm is explained that allows (3) to be enforced when a communication delay separates the master and slave system so that simultaneous information about $\Delta H_{Im}(k)$ and $\Delta H_{Is}(k)$ is unavailable.

[1]With respect to the mathematical notation used in this paper we would like to point out the following. The index k is used to indicate instantaneous values at the sampling instant k and the index $\overline{k}$ is used to indicate variables related to an interval between sampling instants $k-1$ and k.

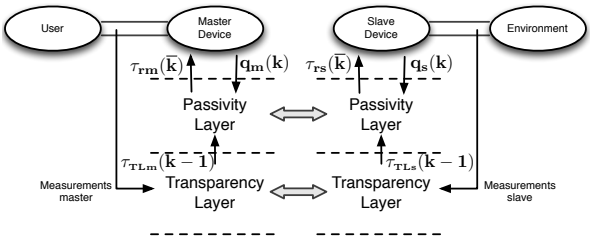

Fig. 2. **Two layer algorithm for bilateral telemanipulation.** The double connections indicate an energy exchange interaction.

As mentioned in Section I the user should not be able to discern the dynamic behavior of the devices and the controllers during operation. This means that with respect to the energy exchange interaction, the following is desired

$$\begin{aligned} H_u &= -H_e \\ \int_{t_0}^{t_1} \tau_u(t)\dot{q}_u(t)dt &= -\int_{t_0}^{t_1} \tau_e(t)\dot{q}_e(t)dt \qquad (4) \end{aligned}$$

where the subscript u and e refer to the interaction point between the user and the master device and between the slave and the remote environment, respectively. H_u and H_e are the energy exchanged between the user and the master device and between the slave device and the remote environment. This means that with respect to the desired energy balance of (4), the device dynamics are still present in the energy balance which the *Passivity Layer* maintains (3), irrespective of the controller in the *Transparency Layer*.

The exchanged energy, $\Delta H_{Is}(k)$ can be divided into three categories:

- Energy injected directly into the environment.
- Energy stored as potential/kinetic energy in the device.
- Energy dissipated due to friction in the device.

Of these three categories the third poses a problem with respect to the energy balances of (3) and (4). The dissipated energy vanishes from the system and is lost. This means that when the slave device is moving a continuous drain of energy at the slave side occurs, forcing the modulated damper at the master side to be activated. Even if the slave is moving in free space, the user will experience the force generated by the modulated damper. Therefore, the activation of the modulated damper decreases the transparency of the system and the decrease in transparency is related to the amount of friction present in the slave device.

III. Friction compensation

In the previous section we have discussed that friction decreases the transparency of the system in the two-layered approach as it poses an additional energy drain. However, as the device is known and does not change much during normal operation, an estimate of this energy, $\overline{\Delta H}_r(k)$, can

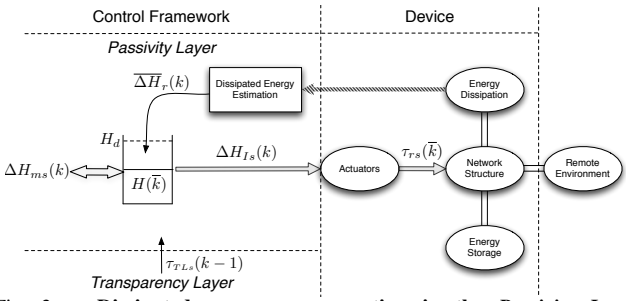

Fig. 3. **Dissipated energy compensation in the *Passivity Layer*:** $\Delta H_{ms}(k)$ represents the two-way energy exchange interaction between the master and slave system. For clarity only the energy flows are depicted in the *Passivity Layer*.

be computed. As long as this estimation is guaranteed to be conservative with respect to the physically dissipated energy it can be reclaimed into the energy tank, Fig. 3. Note that this procedure only works unconditionally for the slave side. When applied to the master side it should be noted that a build-up of energy can occur when the slave is moving in free space.

In order to compensate for the energy lost due to internal friction in the slave system, a model which accurately describes this friction is needed. In literature several friction models have been proposed suitable for various joints and/or materials. Here we will assume that the physical friction can be represented by a model consisting of both coulomb and viscous friction. We furthermore assume that based on a good device characterization the parameters which describe the physical friction are known, or at least a conservative estimate is available. Although the results presented here are specific for the chosen friction model, the procedure of Fig. 3 can contain any number of friction models.

The friction model containing both coulomb and viscous friction is given by

$$F_r(t) = -b_c sgn(\dot{q}(t)) - b_v \dot{q}(t) \tag{5}$$

where b_c and b_v are the coulomb and viscous friction coefficients, respectively.

Using the friction model of (5), the energy dissipated, $\overline{\Delta H}_r(k)$, during a sample period, $\overline{k}$, can be computed *a posteriori* at sample instant k. The input for this computation is the displacement of the slave device that has occurred during the sample period, $\overline{k}$. As this computed energy is added to the energy tank in the *Passivity layer* it needs to be a conservative estimate. Overestimating the dissipated energy would lead to a breakdown of the passivity ensured by the *Passivity Layer*, as "virtual" energy is produced in the energy feedback.

First we will look at the coulomb friction compensation. The power, $P_c(t)$, dissipated due to coulomb friction is

$$P_c(t) = b_c|\dot{q}(t)| \tag{6}$$

The integral of (6) during a sample period gives the dissipated energy. However, it is not possible to detect a change of direction during a sample period. Therefore we must assume that the sample frequency of the control loop is fast enough to capture all the dynamic behavior of the slave device. In that case the energy dissipated by coulomb friction during the previous sample period , $\Delta H_c(k)$, follows directly from the measured displacement as

$$\begin{aligned} \Delta H_c(k) &= \int_{(k-1)T}^{kT} b_c|\dot{q}(t)|dt \\ &= b_c|\Delta q(k)| \end{aligned} \tag{7}$$

The power dissipation due to viscous friction is

$$P_v(t) = b_v \dot{q}(t)^2 \tag{8}$$

As the velocity is not measured at all times, the integral of (8) cannot be explicitly computed. When the average velocity during a sample period is used to compute the viscous friction force, an estimate of the dissipated energy is obtained as

$$\begin{aligned} \overline{\Delta H}_v(k) &= \int_{(k-1)T}^{kT} b_v \frac{\Delta q(k)}{T} \dot{q}(t)dt \\ &= b_v \frac{\Delta q(k)^2}{T} \end{aligned} \tag{9}$$

Using the Cauchy-Schwartz inequality it can be proven that (9) is a lower bound of the integral of (8), as shown by Abbott et al. [1]. This means that estimating the dissipated energy, $\overline{\Delta H}_v(k)$, by viscous friction based on the average velocity is always a conservative estimate of the physically dissipated energy, $\Delta H_v(k)$. Lee et al. [9] have applied (9) for a similar purpose as in this paper. They apply (9) to compute the energy dissipated inside a damped spring-like position controller, whereas in this paper (9) is used to compute the physically dissipated energy in the mechanical structure of the slave device.

IV. Noise Sensitivity

In the previous section we have shown that the dissipated energy by coulomb and viscous friction can be estimated based on a model of the physical friction and a position measurement. Every position measurement suffers from distortion due to noise. In this section we will look into the effects of both Additive White Gaussian Noise (AWGN) and quantization noise on the estimates derived in the previous section.

A. Quantization Noise

Quantization noise occurs due to finite precision with which variables can be transformed from the continuous into the discrete domain. Examples of quantization processes are the number of pulses per rotation for optical rotary encoders and the number of bits of analog-to-digital converters. Here we will assume that all values in a range are mapped onto the boundary values depending on the direction of the signal. The relation between the measured positions, $q_m(k)$, and the physical position, $q(k)$, assuming forward motion is

$$q_m(k) = q(k) - \beta_k \Delta_{SZ} \tag{10}$$

where $\beta \in [0..1)$ and Δ_{SZ} is the step size of the quantization process. This means that the position difference obtained at sample instant k is

$$\Delta q_m = \Delta q(k) - \beta_k \Delta_{SZ} + \beta_{k-1}\Delta_{SZ} \tag{11}$$

In order not to overestimate the true displacement we can compensate for the uncertainty introduced by the quantization of the measured position by assuming the worst case situation in which $\beta_k = 0$ and $\beta_{k-1} \uparrow 1$. This means that the measured displacement is reduced with the step size, Δ_{SZ}, of the quantization process

$$\overline{\Delta q}(k) = sgn(\Delta q(k))(|\Delta q(k)| - \Delta_{SZ}) \tag{12}$$

This compensation technique was also used by Secchi et al. [13] and can be applied for the dissipation estimation functions of both coulomb and viscous friction, (7) and (9), respectively.

B. Additive White Gaussian Noise

Another type of noise often encountered in measurement systems is AWGN. This noise has a gaussian probability density function characterized by a standard deviation, σ_η, is unbiased $\mu_\eta = 0$, and no correlation between consecutive values of the noise. AWGN is often used to represent all kinds of disturbances which cannot precisely be defined, e.g. play, misalignment, thermal effects, finite manufacturing precision etc. [12]

The difference with quantization noise is that it distorts the measurement in the continuous domain. Even if the device is perfectly stationary a displacement will be measured due to this noise vector. Introducing the AWGN noise vector, $\eta(k)$, to the measured position at sample instant k, the measured position difference becomes

$$\Delta q_m(k) = \Delta q + \eta_{\Delta q}(k) \tag{13}$$

where

$$\eta_{\Delta q}(k) = \eta(k) - \eta(k-1) \tag{14}$$

$\eta_{\Delta q}(k)$ is the noise term in the obtained position difference at sample instant k. Combining (13) with the dissipation estimates of (7) and (9) yields

$$\overline{\Delta H}_c(k) = b_c|\Delta q(k) + \eta_{\Delta q}(k)| \tag{15}$$

for the coulomb friction estimate, and

$$\overline{\Delta H}_v(k) = b_v \frac{\Delta q(k)^2 + 2\eta_{\Delta q}(k)\Delta q(k) + \eta_{\Delta q}(k)^2}{T} \tag{16}$$

for the viscous friction estimate. It is observed from (15) and (16) that the addition of AWGN yields non-conservative estimates of the dissipated energy. There is always a positive independent contribution of the noise.

As this noise has a high frequency with respect to the expected physical motions of the device, filtering is an option to reduce its effect. Filtering however will never remove all of the noise and higher-order filters can introduce a significant amount of phase-lag which will interfere with the other processes of the *Passivity Layer*. However, this negative noise effect can be compensated without filtering. The major problematic noise additions in (15) and (16) are the absolute and quadratic terms, which can be regarded as being independent of the actual displacement. Even though the instantaneous value of $\eta_{\Delta q}(k)$ cannot be determined, the long term contribution to (15) and (16) is determined by the probability density function, $f(x)$, characterizing the AWGN. Using this probability density function the average noise contribution to (15) and (16) can be determined.

The probability density function, $f(x)$, of AWGN [6] is

$$f(x) = \frac{1}{\sqrt{2\pi\sigma_\eta^2}} e^{\frac{-x^2}{2\sigma_\eta^2}} \tag{17}$$

where σ_η is the standard deviation of the noise. The average value of this distribution when the absolute value of the noise is considered can be obtained by computing

$$\begin{aligned} \mu_{|\eta|} &= \frac{1}{\sqrt{2\pi\sigma_\eta^2}} \int_0^\infty x e^{\frac{-x^2}{2\sigma_\eta^2}} dx \\ &= \frac{\sigma_\eta}{\sqrt{2\pi}} \end{aligned} \tag{18}$$

The average value can also be computed for the quadratic noise

$$\begin{aligned} \mu_{\eta^2} &= \frac{1}{\sqrt{2\pi\sigma_\eta^2}} \int_{-\infty}^\infty x^2 e^{\frac{-x^2}{2\sigma_\eta^2}} dx \\ &= \sigma_\eta^2 \end{aligned} \tag{19}$$

Using (18) and (19) and considering that the average value of $\eta(k)\eta(k-1)$ is zero it follows that

$$\begin{aligned} \sum_{k=1}^{n} |\eta_{\Delta q}(k)| &\approx \sum_{k=1}^{n} 2\mu_{|\eta|} \\ \sum_{k=1}^{n} \eta_{\Delta q}(k)^2 &\approx \sum_{k=1}^{n} 2\mu_{\eta^2} \end{aligned} \tag{20}$$

if n is large enough.

We can use (20) in (15) and (16) to compensate for the non-conservative influence of the AWGN.

C. Energy dissipation estimation with noise compensation

In the previous sections the influence of two types of measurement noise on the energy dissipation estimation functions of Section III was discussed and a compensation method was proposed. Each type of noise was treated independently, but in practice the quantization procedure will also influence the amount of the AWGN that is present in the measurement. Applying the derived solutions when both types of noise are present will make the estimation conservative. As this is desired it is considered not to be a problem.

Application of (12) and (20) to the estimation functions (7) and (9) yield the following noise compensated estimation functions

$$\begin{aligned} \overline{\Delta H}_r(k) &= \overline{\Delta H}_c(k) + \overline{\Delta H}_v(k) \\ &= b_c(|\overline{\Delta q}(k)| - 2\mu_{|\eta|}) + b_v \frac{\overline{\Delta q(k)}^2 - 2\mu_{\eta^2}}{\Delta T} \end{aligned} \tag{21}$$

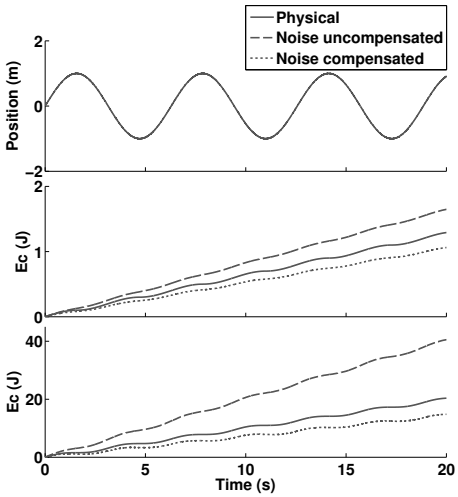

Fig. 4. **Energy dissipated by coulomb and viscous friction estimation.** The plots show that the energy estimation without noise compensation can largely differ from the physically dissipated energy. Using the compensation technique a conservative estimate is obtained for both types of friction.

where $\overline{\Delta H}_r(k)$ is the combined estimated dissipated energy. As the noise compensation can be too conservative when the device is not moving the following lower bound is enforced

$$\sum_{k=1}^{n} \overline{\Delta H}_r(k) \geq 0 \tag{22}$$

which means that the estimated dissipated energy is always at least equal to zero.

Fig. 4 shows the estimated dissipated energy for a general sinusoidal motion applied to a damper with arbitrarily chosen friction coefficients $b_c = 0.1$ and $b_v = 2$, respectively. The regular estimation technique, given by (7) and (9), and the noise compensated technique of (21) are implemented. The energy estimation procedures are executed at a sample frequency of 1 kHz Both AWGN and quantization are applied to the position measurement. A quantizer with step size $9.58 \times 10^{-5} m$ was applied and the AWGN had a standard deviation $\sigma_\eta = 5 \times 10^{-4}$. It is seen that without the noise compensation the dissipated energy by both coulomb and viscous friction is largely overestimated. The energy dissipated by viscous friction is especially susceptible to noise influence and is overestimated by approximately 100% for this small noise vector. Fig. 4 also shows that the noise compensated estimation functions are indeed conservative.

V. Example

In Section IV the negative influence of two types of measurement noise on the dissipated energy estimation functions was discussed and a compensation algorithm was proposed. In this section we will apply this compensation algorithm at the slave side into a full simulation of the framework of Section II.

A. Model

We will consider the situation where the user is executing a sinusoidal motion with the master device. The master and slave devices are modeled by

$$\begin{aligned} \tau_u(t) + \tau_{rm}(t) &= m_m \ddot{q}_m(t) + b_{vm}\dot{q}_m(t) \\ \tau_e(t) + \tau_{rs}(t) &= m_s \ddot{q}_s(t) + b_{cs} sgn(\dot{q}_s(t)) + b_{vs}\dot{q}_s(t) \end{aligned} \tag{23}$$

where m_*, b_{c*}, and b_{v*} represent the mass, coulomb friction coefficient, and viscous friction coefficient, respectively, of either the master or slave device. The force exerted by the user $\tau_u(t)$ is such that

$$q_m(t) = 0.25 sin(t) \tag{24}$$

The remote environment consists of a soft viscoelastic material located at position q_w. The interaction force with this material, $\tau_e(t)$ is given by

$$\begin{aligned} p_e(t) &= q_s(t) - q_w \\ \tau_e(t) &= \begin{cases} -k_{pe}p_e(t) - k_{de}|p_e(t)|\dot{p}_e(t) & \text{if } p_e(t) < 0 \\ 0 & \text{otherwise} \end{cases} \end{aligned} \tag{25}$$

where $p_e(t)$ is the penetration of the slave device into the viscoelastic material and k_{pe} and k_{de} are the stiffness and damping of the material, respectively.

In the *Transparency Layer* a position-force controller is implemented. A PD-controller is implemented at the slave side to synchronize the motion of the slave device with that of the master and the measured interaction force at the slave side is set as desired torque to be applied to the master device

$$\begin{aligned} \tau_{TLs}(k) &= k_{ps}(q_m(k) - q_s(k)) - k_{ds}\dot{q}_s(k) \\ \tau_{TLm}(k) &= \tau_e(k) \end{aligned} \tag{26}$$

The communication channel connecting the master and slave device in this example is ideal (lossless and zero time delay). Therefore, the energy tanks at the master and slave side in the *Passivity Layer* are combined into a single energy tank. For this example no additional limiting functions have been implemented in the *Passivity Layer*. Noise with the same characteristics as in Section IV-C is added to the position measurement.

TABLE I
PARAMETER VALUES USED IN THE SIMULATION

Parameter	Value	Parameter	Value
m_m	0.1 kg	m_s	0.1 kg
b_{vm}	0.1 Ns/m	b_{cs}	0.1 N
b_{vs}	2 Ns/m	q_w	-0.2 m
k_{ps}	100 N/m	k_{ds}	10 Ns/m
H_d	0.1 J	α	100
k_{pe}	20 N/m	k_{de}	100 Ns/m

B. Simulation results

The simulations have been carried out with the simulation program 20-sim [3]. The two-layered control framework is executed at a sample frequency of $1kHz$. The parameter values used in the simulation are listed in Table I. The physical meaning of the parameters has been discussed in Section II and V-A

Two simulations have been performed. In the first, the telemanipulation system is operating without the energy dissipation compensation proposed in Section IV. In the

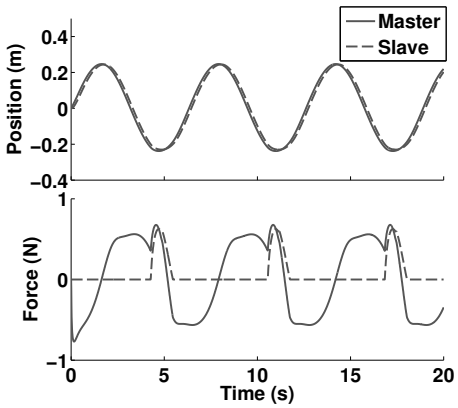

Fig. 5. **System response of the bilateral telemanipulation system without friction compensation:** The modulated damper is continuously activated to compensate for the energy dissipated by the internal friction of the slave device causing the interaction force to be masked.

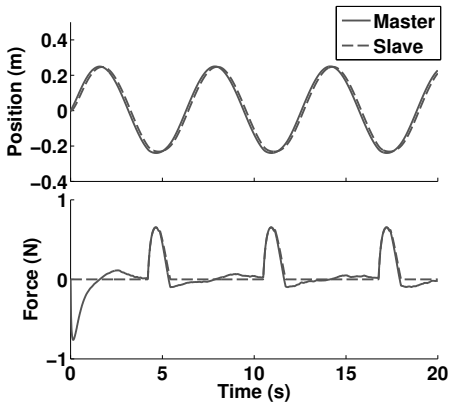

Fig. 6. **System response of the bilateral telemanipulation system with friction compensation:** The interaction forces are now discernible at the master side.

second simulation the user is executing the same motion, but now with the dissipated energy compensation enabled.

Fig. 5 depicts the response of the telemanipulation system without the energy dissipation compensation. The friction at the slave side causes a position lag with respect to the position of the master device. A large difference between the interaction force at the slave side and the feedback force at the master side is visible. This force difference indicates that the modulated damper of (1) is continuously activated to compensate for the energy dissipated internally in the slave device. The peak of the interaction force at the slave side can be seen in the feedback force at the master system, but it is unlikely that the user will be able to clearly discern this force during operation.

Fig. 6 shows the system response when the dissipated energy compensation is enabled. The position lag between master and slave is still present as the controller in the *Transparency Layer* is not optimized to deal with the friction forces in the slave system. Now the energy dissipated by that friction is reclaimed in the *Passivity Layer* and no longer has to be extracted from the user by the modulated damper. The interaction forces between the slave device and the remote environment are now much more accurately reflected by the master device to the user. This indicates a significant increase in obtained transparency. As discussed in Section IV the energy estimation is conservative and as a result it is not entirely reclaimed. Therefore, the modulated damper is still lightly activated to compensate for the difference between the estimated and the physically dissipated energy.

VI. Conclusions and Future Work

A compensation technique was proposed for the energy dissipated by physical friction in the slave device of a time-domain passive telemanipulation system. By reclaiming this energy the transparency of the system is increased. An analysis was performed showing that measurement noise, especially AWGN, has an adverse effect on the regular estimation functions leading to overestimation of the dissipated energy. It is shown that given the probability distribution of the noise, a conservative estimate of the dissipated energy can be obtained without filtering.

A clear increase in obtained transparency is obtained in a simulation of a time-domain passive bilateral controller. However, the introduced compensation technique is not limited to the used two-layered framework and can be applied in any time-domain passivity based algorithm.

Future work will focus on implementing this compensation technique on a physical telemanipulation system with high internal friction to investigate the increase in obtained transparency.

References

[1] J. Abbott and A. Okamura, "Effects of position quantization and sampling rate on virtual-wall passivity," *IEEE Trans. Robotics*, vol. 21, no. 5, pp. 952–964, 2005.

[2] L. Bernstein, D. Lawrence, and L. Pao, "Friction modeling and compensation for haptic interfaces," *Proc. World Haptics*, pp. 290–295, 2005.

[3] Controllab Products B.V., "20-sim version 4.1," http://www.20sim.com/, 2010.

[4] G. Ferretti, G. Magnani, and P. Rocco, "Impedance control for elastic joints industrial manipulators," *IEEE Trans. Robotics and Automation*, vol. 20, no. 3, pp. 488–498, 2004.

[5] M. Franken, S. Stramigioli, R. Reilink, C. Secchi, and A. Macchelli, "Bridging the gap between passivity and transparency," *Proc. Robotics: Science and Systems*, June 2009.

[6] S. Haykin, *An Introduction to Analog and Digital Communications*. John Wiley & Sons, Inc., 1989.

[7] V. Hayward and M. Cruz-Hernandez, *Experimental Robotics IV*, ser. Lecture Notes in Control and information Systems. Springer-Verlag, 1997, vol. 223, ch. Parameter sensitivity analysis for design and control of tendon transmissions, pp. 241–252.

[8] D. Lawrence, "Stability and transparency in bilateral teleoperation," *IEEE Trans. Robotics and Automation*, vol. 9, no. 5, pp. 624–637, 1993.

[9] D. J. Lee and K. Huang, "Passive position feedback over packet-switching communication network with varying-delay and packet-loss," *Proc. Symp. of Haptic Interfaces for Virtual Environments and Teleoperator Systems*, pp. 335–342, 2008.

[10] M. Mahvash and A. Okamura, "Friction compensation for enhancing transparency of a teleoperator with compliant transmission," *IEEE Trans. Robotics*, vol. 23, pp. 1240–1246, 2007.

[11] J.-H. Ryu, D.-S. Kwon, and B. Hannaford, "Stable teleoperation with time-domain passivity control," *IEEE Trans. Robotics and Automation*, vol. 20, no. 2, pp. 365–373, 2004.

[12] L. Sanchez-Brea and T. Morlanes, "Metrological errors in optical encoders," *Meas. Sci. Technol.*, vol. 19, no. 11, pp. 1–8, 2008.

[13] C. Secchi, S. Stramigioli, and C. Fantuzzi, *Control of interactive robotic interfaces*, ser. Springer Tracts in Advanced Robotics vol. 29. New York: Springer-Verlag, 2006.

[14] S. Stramigioli, C. Secchi, A. van der Schaft, and C. Fantuzzi, "A novel theory for sampled data system passivity," *Proc. IEEE/RSJ Int. Conf. Intelligent Robots and Systems*, pp. 1936–1941, 2002.